Retinal Trauma

27

Carsten H. Meyer, Fernando M. Penha,
Michel E. Farah, and Peter Kroll

Contents

C.H. Meyer, MD, FEBO, FMH (✉)
Department of Ophthalmology, Pallas Klinik, Aarau, Switzerland
e-mail: meyer_eye@yahoo.com

F.M. Penha, MD, PhD
Bascom Palmer Eye Institute, University of Miami, Miami, FL, USA

M.E. Farah, MD
Department of Ophthalmology, Federal University of São Paulo, São Paulo, Brazil

P. Kroll, MD
Department of Ophthalmology, Philipps University, Marburg, Germany

27.1 Introduction

Non-penetrating or closed-globe injuries represent 50–80 % of traumatic eye injuries. Generally, the most affected population is the man under 30 years old. It may occur by several mechanisms thus damaging a variety of different retinal structures. The Ocular Trauma Classification Group defined a standardized classification for frequently used terms based on standard terminology and features of ocular injuries that have demonstrated prognostic significance. In a closed-globe injury, the eye wall does not have a full-thickness wound, and the mechanism of injury may be grouped into two main categories: the direct (anterior) type occurring at the site of the impact and an indirect (posterior) type at the contrecoup injury, which is more commonly found. Several groups investigated the mechanical impact of blunt ocular trauma and reported theories how defined anatomical structures can be damaged (Fig. 27.1). After a traumatic event, the vision can be unaffected or completely lost, depending on the location of the damaged anatomical structure, e.g., choroidal vessels, choriocapillaris, Bruch's membrane, retinal pigment epithelium (RPE), and neuroretina (Berg et al. 1989; Mennel et al. 2004; Williams et al. 1990).

The following chapter demonstrates a variety of closed-globe injuries on time and spectral

C.H. Meyer et al. (eds.), *Spectral Domain Optical Coherence Tomography in Macular Diseases*,
DOI 10.1007/978-81-322-3610-8_27

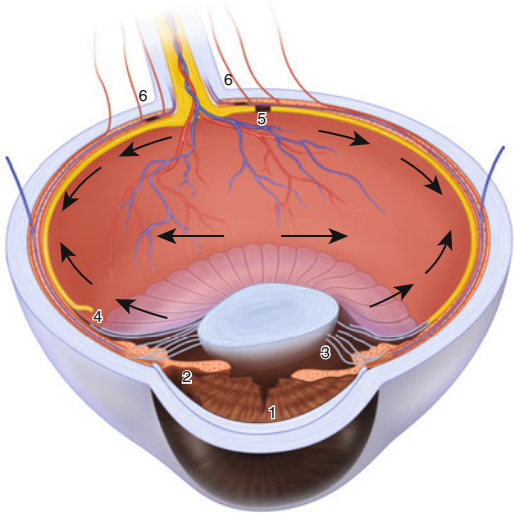

Fig. 27.1 Non-penetrating or closed-globe injuries may occur by several mechanisms thus damaging a variety of different retinal structures including the iris (*1*), trabecular mash work (*2*), lens fibers (*3*), retina (*4*), posterior pole (*5*), or optic nerve with the posterior ciliary vessels (*6*)

domain optical coherent tomography (OCT), fluorescein angiography (FA), autofluorescence (AF), and fundus photography.

27.2 Choroidal Folds

Choroidal folds were first described by Nettleship in 1884 and were initially considered as foldings of the entire retina (Nettleship 1884). They are visible striae at the posterior pole that radiate across the macula arranged in a parallel and horizontal fashion as dark and light lines. Later Norton investigated the typical fluorescein angiographic (FA) appearance and defined a clear distinction between choroidal and retinal folds (Norton 1969). The anatomical structure of choroidal folds can be explained by the typical fluorescein pattern traversing the folded choroidal vessels. Hyperfluorescent streaks occur in the early arteriovenous phase and persist throughout the late venous phase with no leakage. A stretching and atrophy of the RPE induce an increased filling of the choriocapillaris overlying this peak of the choroidal fold. Hypofluorescent streaks are on the bases of inclinated RPE in the valley of the fold, resulting to a compression of the pigment-containing base of the RPE cells and blockage of the underlying choroidal fluorescence. Histological studies confirmed a folding at the level of the RPE, Bruch's membrane, and choroid giving the retina above a "brain-like" configuration. Cross-sectional imaging by computer tomography (CT) or B-scan ultrasonography reveals an abnormal flattening of the posterior pole, a thickening of the sclera, and a consecutive axial shortening of the globe (Dailey et al. 1986). This characteristic picture is associated with a variety of orbital and ocular conditions including trauma, hypotony, orbital tumors, thyroid disease, papillitis, or uveal effusion syndrome.

Color fundus picture (Fig. 27.2a) and fluorescein traversing the folded choroidal vessels demonstrated hyperfluorescent streaks in the early and late phase with no signs of leakage, while adjacent hypofluorescent streaks remained dark throughout the entire angiography. In vivo measurements by OCT determined a significant folding of the hyperreflective RPE-choriocapillaris complex (Fig. 27.2b) in the papillomacular area. The thickness, reflectivity, and surface contour of the retina appeared within normal limits.

Differently patients with ocular hypotony may face severe impaired vision with metamorphopsia. On fundus examination there is a significant tortuous beading of the retinal and venous vessels (Fig. 27.3a). Fluorescein angiography (FA) demonstrates a fussy fluorescence in the early and late phase (Fig. 27.3b). OCT shows a mountain-like folding of the entire retina with moderate hyporeflective areas in the subretinal space corresponding with subretinal fluid (Fig. 27.3c). Between the RPE and the sclera, there are flat large areas corresponding with choroidal fluid.

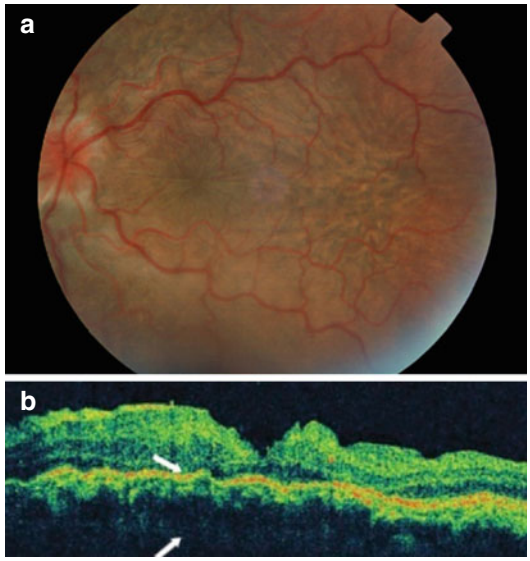

Fig. 27.2 Choroidal folds. (**a**) In the late venous phase of the fluorescein angiography, there are multiple parallel and horizontal lines of different fluorescence in the macular area. The hyperfluorescent streaks persist with no leakage and are caused by an increased filling of the choriocapillaris overlying the peak of the choroidal fold. The hypofluorescent streaks are in the valley of the fold, where the compressed RPE blocks the underlying choroidal fluorescence. (**b**) The vertical OCT scan of the choroidal folds in the papillomacular area. The inner surface of the retina is flattened by image analysis using Adobe Photoshop, so that the choroidal folds become more prominent. The neuroretina in the papillomacular bundle has a moderate reflectivity and normal thickness of approximately 225 μm. There is no intraretinal or subretinal fluid. The folded hyperreflective band, in red to white colors, corresponds to the RPE-choriocapillaris complex and is firmly attached to the underlying sclera, with no signs of pigment epithelium detachment (PED). Each fold has a height of approximately 45 μm. The dark and hyporeflective spots in the deep scleral layer under each fold (*white arrows*) may either correspond to compressed tissue or shadowing of the folded RPE-choriocapillaris complex

27.3 Commotio Retinae

Commotio retinae are defined as a transient gray-white opacification at the level of the deep sensory retina occurring after blunt ocular trauma, and it was first described by Berlin in 1873 (Berlin 1873). The whitening and elevation of the retina appear immediately after a trauma and can be limited to the central retina although it may even involve extensive areas of the peripheral retina progressing to retinal necrosis and chorioretinitis sclopetaria (Hesse et al. 1996).

Commotio retinae are grouped in two variations: a milder type (retinal concussion) with less dramatic gray-white changes and no visible pigment alterations, which later may progress to scarring. The more severe type (retinal contusion or chorioretinitis sclopetaria) can occur anterior at the point of impact (coup) or posterior at the remote impact site (contrecoup). A coup damage is therefore caused by local trauma directly at the site of impact, while a contusive contrecoup injury occurs at the opposite site of the blunt trauma creating damage at tissue interfaces. The consecutive whitening is more severe and a creamy discoloration of the RPE appears within 48 h after the injury. Fluorescein angiography typically demonstrates an alternated retinal vascular permeability, a bright leakage due to a partial breakdown of the outer blood-retina barrier at the level of the RPE. Visual acuity may be transiently or permanently reduced. The visual prognosis is good if the damaged location is outside the fovea. However, if the fovea is involved, vision loss may maintain permanently (Fig. 27.4) (Hesse et al. 1996; Sipperley et al. 1978).

The clinicopathologic features of retinal contusion or chorioretinitis sclopetaria include direct traumatic chorioretinal damage followed by marked fibrovascular proliferation with variable replacement of vascular and neuroretinal tissue (Fig. 27.4a). A visible retinal opacity at the site of the contrecoup injury is considered to be a severe injury. It may later progress to a "salt-and-pepper" appearance accompanied by a hypofluorescence on fluorescein angiography. The chorioretinal circulation disturbance corresponds with a delayed filling and narrowing of the choroidal veins and changes in choroidal vasculature causing obstruction and occlusion of the choriocapillaris (Fig. 27.4b, c). The breakdown of the outer blood-retina barrier in the RPE may increase permeability of the choriocapillaris.

Histopathologic studies demonstrated a partial loss of the nerve fiber and ganglion cell layers and loss of the photoreceptors with hypertrophy and hyperplasia of the RPE. Although the sclera

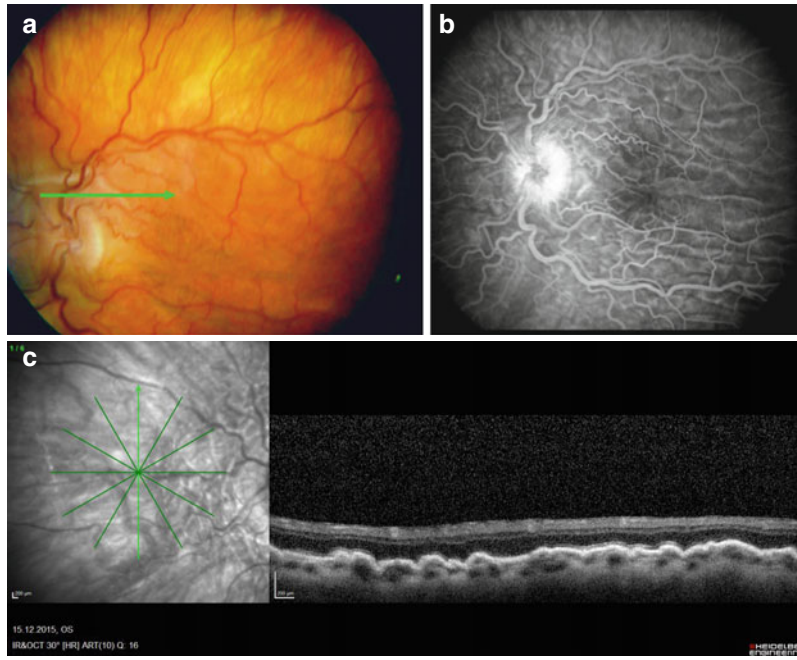

Fig. 27.3 (**a**) Fundus image of the right eye in patients with severe hypotony after blunt ocular trauma. Funduscopy demonstrates a chorioretinal folding of the entire retina (*green arrow*). (**b**) Fluorescein angiography demonstrates a moderate elevation of the retina with mild leakage. (**c**) On OCT there is a significant folding of the entire neuroretina (**X**) with some hyporeflective areas under the retina corresponding with subretinal fluid. Under the hyperreflective RPE-choriocapillaris complex, there is a broad hyperreflective area (*) presenting a second fluid compartment in the choroid adjacent to the sclera

and a long posterior ciliary nerve remained intact, a marked ingrowth of fibrovascular tissue may be extended from the choroid into the subretinal space where it was covered by retinal pigment epithelium. On OCT there is a marked thinning of the neuroretina in the affected area compared to the unaffected adjacent areas (Fig. 27.4d, f) (Dubovy et al. 1997; Pahor 2000).

There have been conflicting reports on histopathologic features of Berlin's edema or commotio retinae. Although Berlin originally hypothesized that the loss of the outer retinal transparency may relate to an extracellular edema, the origin and underlying pathogenesis remain controversial. Several postmortem studies on human and animal eyes confirmed a disruption of photoreceptor outer segments followed by phagocytosis of fragmented outer segments by the retinal pigment epithelium (RPE), while some authors reported a direct damage to the neurosensory retina as seen by swelling of Müller food processes and mitochondria in the nerve fiber layer. The gross anatomy revealed swollen inner segments with mitochondrial deposits of resembling calcium, indicating an increased permeability of the plasma membranes. The blunt ocular trauma may generate mechanical contrecoup distortion of the retina via vitreoretinal attachments. Mansour et al. hypothesized that hydraulic forces stretch the neuroretina at the level of the outer segments, while intact Müller cells hold the rest of the retina together (Mansour et al. 1992).

In vivo measurements by OCT revealed a traumatic lesion at the level of the photoreceptor-RPE complex, disclosing a detached sensory retina with fluid in the subretinal space. The reflectivity of the neuroretinal tissue was reduced and the architecture less compact. The neuroretina, held together by the Müller food processes, appears to be intact up to the photoreceptors. The uncommon hyperreflective inner retinal band possibly represents the photoreceptor inner segments, with less reflective outer segments underneath and in the subretinal space. Although the neuroretinal thickness was increased, the foveolar indentation remained still visible (Fig. 27.5b). Fundus biomicroscopy revealed a mild retinal

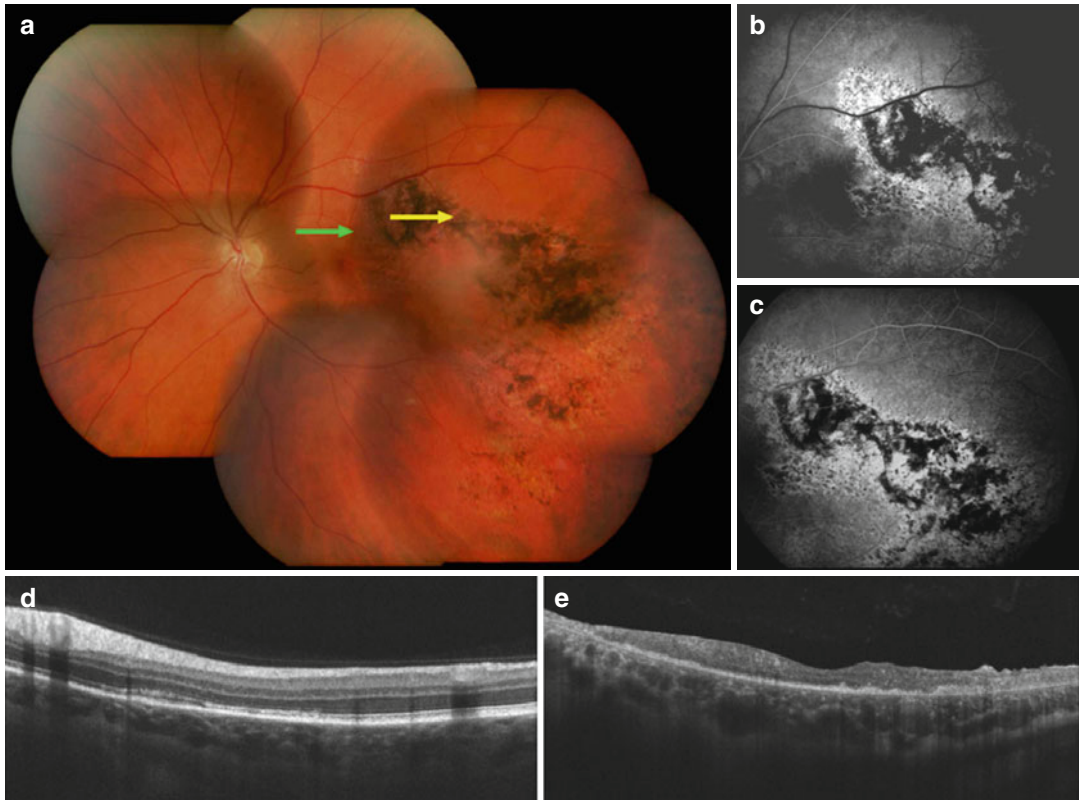

Fig. 27.4 Chorioretinitis sclopetaria. (**a**) Fundus image of the left posterior pole resulting from a localized destruction of both the retina and choroid (*yellow arrow*) with connective tissue proliferation adjacent to the impact site (*green arrow*). (**b**, **c**) Fluorescein angiography shows irregular filling of the choriocapillaris and partially obstructed by connective tissue plaques. (**d**, **e**) SD-OCT showing marked thinning of the entire neuroretina

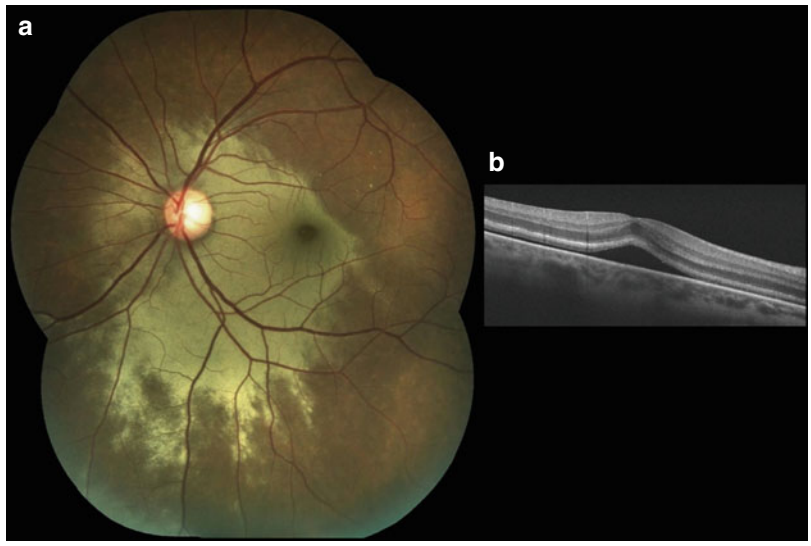

Fig. 27.5 (**a**) Fundus image of the left posterior pole showing dull foveal reflex and mild retinal elevation in the papillomacular region. (**b**) Horizontal OCT scan in the papillomacular area demonstrates a detachment of the entire neuroretina with hyporeflective space underneath, corresponding with subretinal fluid

elevation at the level of neurosensory retina and the RPE in the fovea with white concentric lines (Fig. 27.5b). The RPE phagocytoses damaged the outer segments and restore central vision within weeks. We determined a full anatomical and functional recovery of the macular lesion within 3 months. The patient's vision returned to 20/20 OU 5 months later (Meyer et al. 2003a).

Another complication that may occur after commotio retinae is the traumatic pigment epitheliopathy. It is possible to identify RPE atrophy with areas of discoloration and pigment clumping associated with patchy lesions, which represented post-traumatic pigment epitheliopathy. Fundus autofluorescence (FAF) examination demonstrated a well-defined reduced FAF patchy area with interposed granular increased autofluorescent areas in regions of the epitheliopathy (Fig. 27.6). OCT showed an area of increased reflectivity beneath the choriocapillaris/RPE complex and focal thinning of the retina. We also demonstrated the functional damage of traumatic pigment epitheliopathy using Humphrey's computerized visual field in one patient and compared these findings to autofluorescence imaging, which correlated to the area of decreased sensitivity of the visual field (Fig. 27.7). Therefore, alterations in autofluorescent pattern in these patients may be an indirect indication of the function of the retina and RPE and could be suggestive of poor prognosis in some cases of commotio retinae.

27.4 Choroidal Rupture

Choroidal rupture, first described by von Graefe in 1854, is a breach of Bruch's membrane, the choroid, and the RPE secondary to a blunt ocular trauma (Von Graefe 1854). They can be divided into two main categories: a direct (anterior) type occurring at the site of the impact is oriented parallel to the ora serrata. Indirect ruptures, which are more common, occur predominantly at the

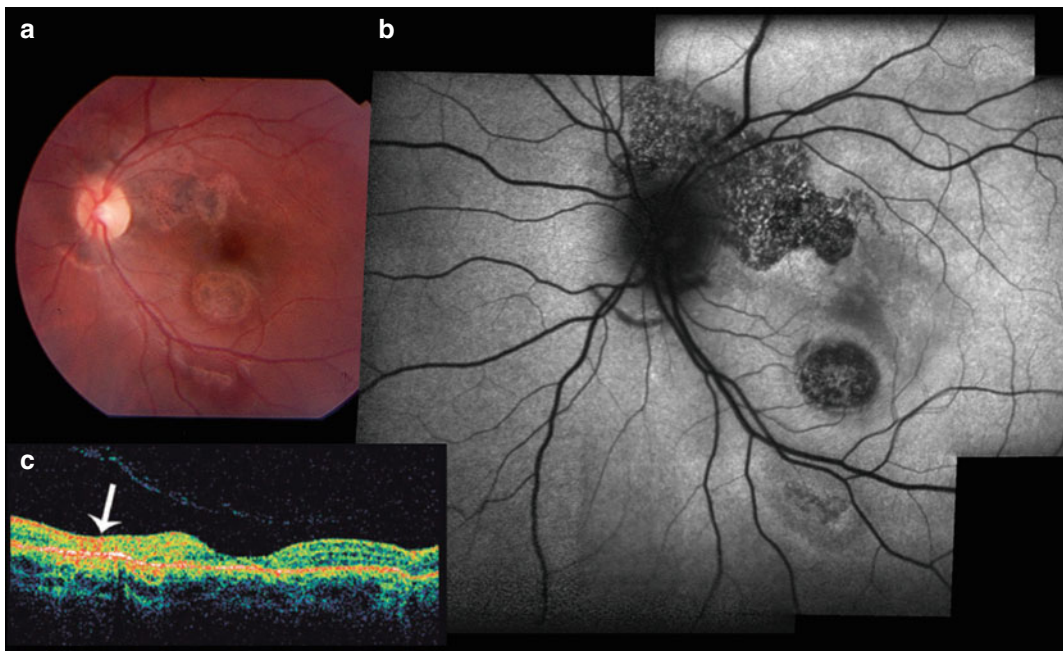

Fig. 27.6 (**a**) Color fundus picture showing peripapillary retinal pigment epithelium (RPE) atrophy with areas of discoloration and pigment clumping (Courtesy of Dr Daniel Lavinsky). (**b**) Fundus autofluorescence (FAF) demonstrates reduced FAF area in the same region of RPE atrophy with an increased granular autofluorescent pattern inside the lesion (Courtesy of Dr Daniel Lavinsky). (**c**) Optical coherence tomography (OCT) shows increased reflectivity of the choriocapillaris/RPE complex and local thinning of the retina (*white arrow*) (Courtesy of Dr Daniel Lavinsky)

posterior pole away from the site of impact. The rupture is here usually crescent shaped and concentrically aligned to the optic disk, with the convexity away from the optic disk. The majority (82 %) of ruptures run temporal to the optic disk may involve the macula.

Mechanical and vascular mechanisms are the two most frequently cited hypotheses explaining the damages in choroidal ruptures. During a closed-globe injury, the eyeball is first mechanically compressed and then rapidly hyperextended. The sclera's tensile strength resists this compression. The retina is elastic and stretches during such an injury. However, Bruch's membrane breaks because it does not have sufficient tensile strength or elasticity. The choriocapillaris is injured and bleeds into the sub-RPE and/or subretinal space. Such hemorrhage may hide the choroidal rupture initially. Over days, the blood clears and a whitish/yellowish, curvilinear, crescent-shaped subretinal streak is visible and concentric to the optic disk. Between 5 and 10 % of all blunt ocular trauma lead to indirect choroidal ruptures (Wagemann 1902).If there is a large amount of hemorrhage, surgery may be indicated with vitrectomy subretinal tissue plasminogen activator and gas displacement.

Over time, choroidal neovascularization (CNV) can develop. In most cases, the CNV involutes over time. Secretan et al. demonstrated that ruptures greater than 4000 μm in length and located within 1500 μm of the center of the fovea are more frequently associated with CNV (Secretan et al. 1998). In about 30 %, the CNV may recur, with a serous or hemorrhagic pigment epithelial detachment, anytime following the

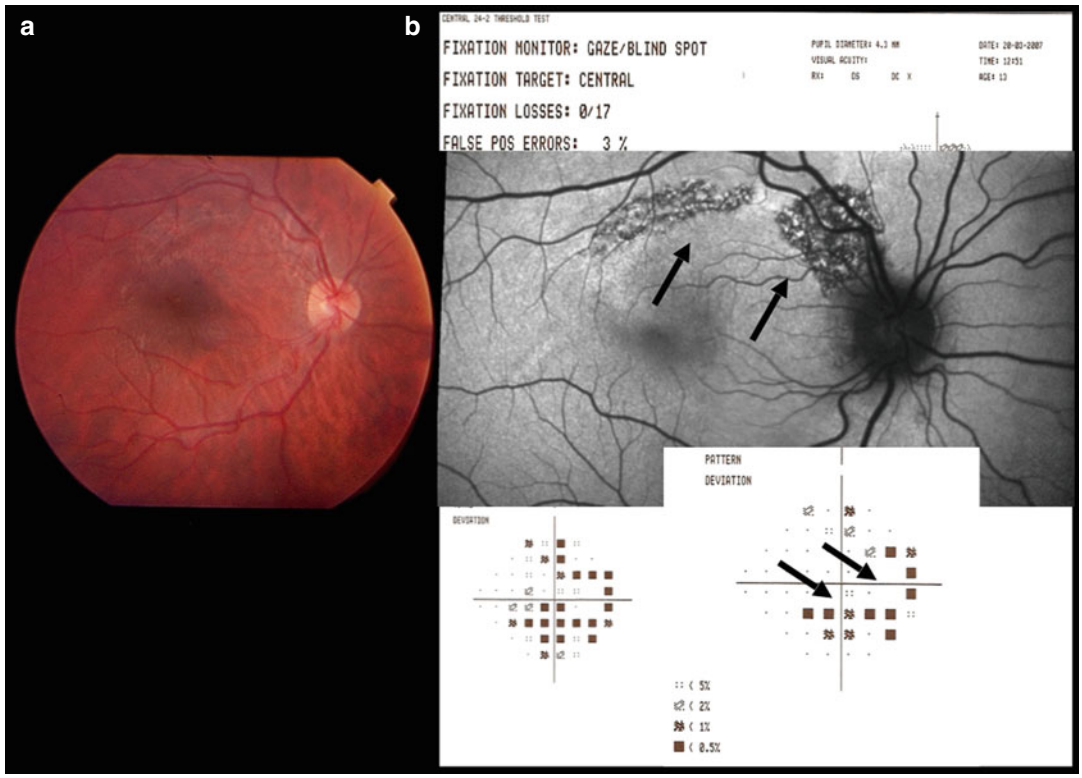

Fig. 27.7 (**a**) Ocular fundus photography of the right eye showing a mild pigmentary change at the temporal superior arcade (Courtesy of Dr Daniel Lavinsky). (**b**) Fundus autofluorescence (FAF) demonstrates two reduced autofluorescent areas with increased autofluorescent granular areas (*arrow*). Humphrey's 24-2 SITA-standard strategy perimetry demonstrates acceptable reliability scores and a significant decrease in the sensitivity of lower nasal fields, corresponding to the superior temporal pigment epitheliopathy evident on autofluorescence (*arrow*) (Courtesy of Dr Daniel Lavinsky)

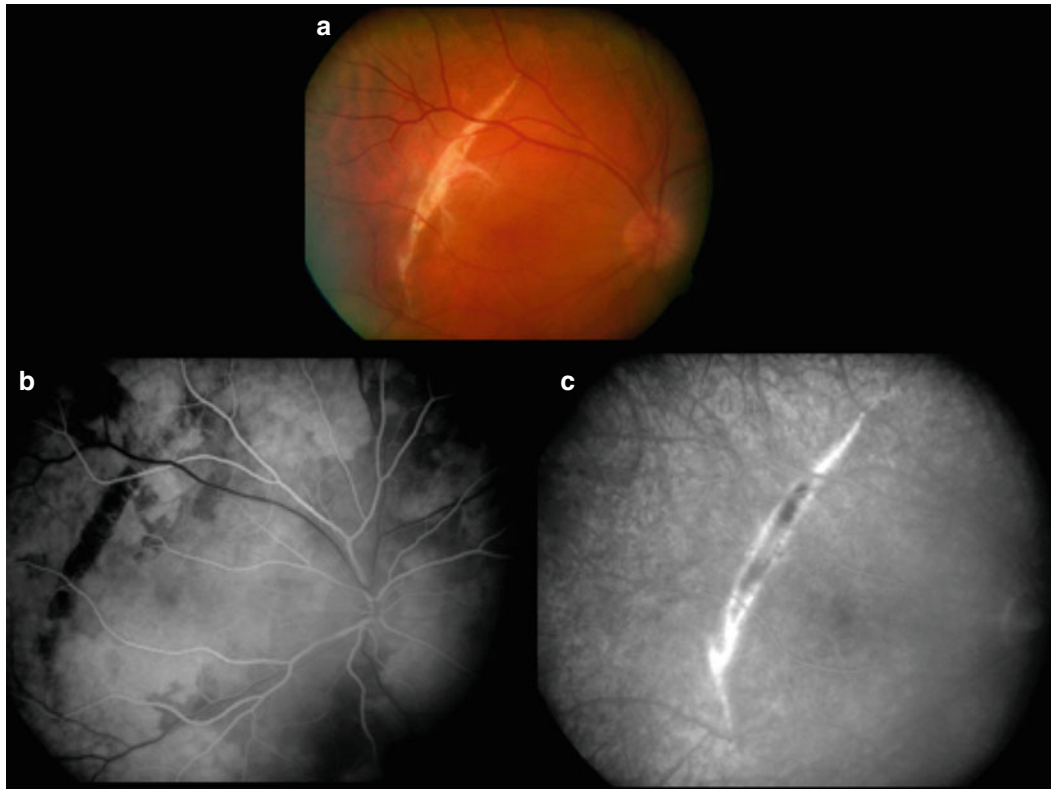

Fig. 27.8 Choroidal rupture. (**a**) Fundus image demonstrates a white crescent-like rupture of the choroid in the superior temporal quadrant. (**b**) Fluorescein angiography early phase showing an incomplete filling of the choroidal vasculature. In the area of the choroidal rupture, there is a dark hypofluorescence visible consistent with the rupture and loss of choroidal vessels. (**c**) Fluorescein angiography late phase showing sharp crescent-like hyperfluorescence due to leakage of choroidal vessels and a window defect at the choroidal rupture

formation of the choroidal rupture. If the rupture or CNV does not involve the foveal center, vision may not be affected. Late complications may also include migration of RPE cells, ERM (epiretinal membrane) formation, loss of photoreceptors, optic atrophy, and retinal detachment.

Fluorescein angiography demonstrates a crescent-shaped delay filling at the site of the choroidal rupture. Early on there is a hypoperfusion of the choroidal artery. Evidence of the choroidal rupture hyperfluorescent streak occurred in the late phase of the FA at the site of the choroidal rupture (Fig. 27.8a–c). In another case it is possible to observe besides the choroidal rupture and progressive hyperfluorescent lesion in the macular area corresponding to a secondary CNV (Fig. 27.9a–d). ICG may also disclose a hypofluorescent rim along the choroidal veins as signs of an increased permeability of the choriocapillaris. These feeder vessels seem to have a greater caliber and a higher tendency to proliferate and are therefore more resistant to photodynamic therapy (PDT) and selective feeder vessel treatment as demonstrated by us previously (Mennel et al. 2005). More recently some case reports have been published treating this secondary CNV with anti-VEGF therapy such as bevacizumab or ranibizumab (Janknecht 2011; Piermarocchi and BenettiE 2011).

SD-OCT highlights the cross-sectional features of choroidal ruptures. The first case demonstrated a mounted subretinal lesion corresponding with fibrovascular scar tissue and some fluid underneath and inside the retina showing an active CNV secondary to a choroidal rupture (Fig. 27.9e–f).

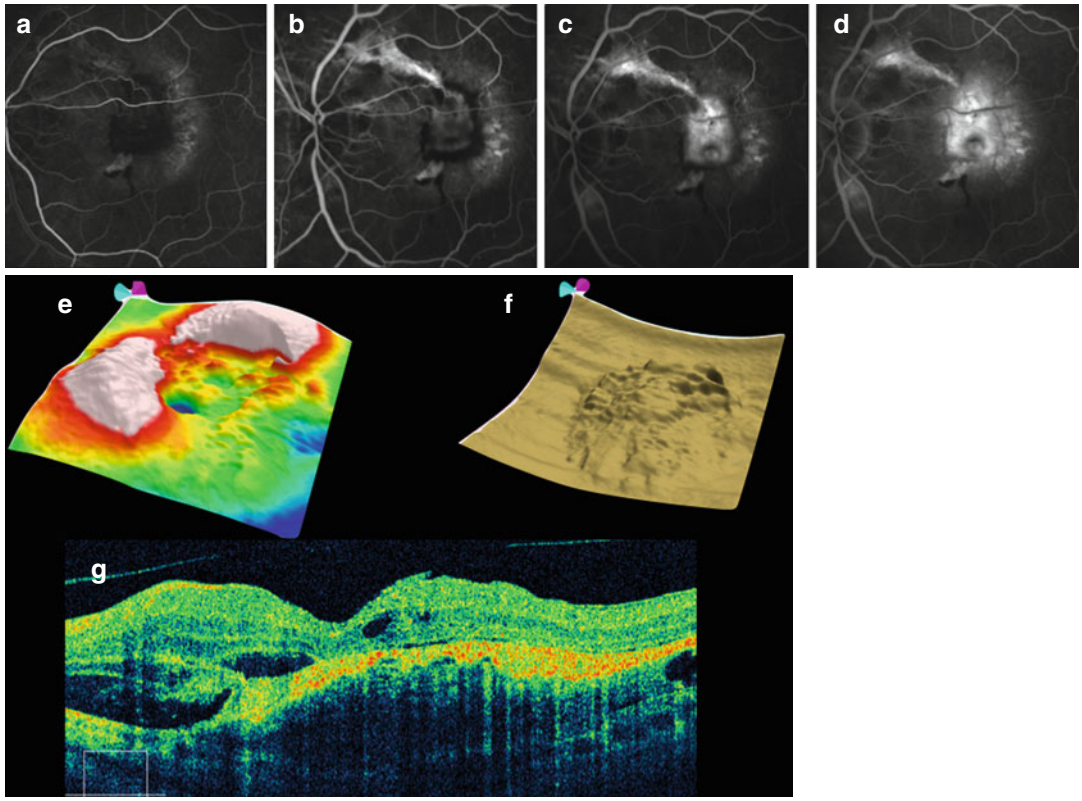

Fig. 27.9 Choroidal rupture. (**a**) Fluorescein angiography showing crescent-like hyperfluorescent lesion in the superior temporal region corresponding to the choroidal rupture. (**b**–**d**) Serial fluorescein angiography shows progressive hyperfluorescent lesion in the macular area corresponding to a secondary choroidal neovascularization (CNV). (**e**) The retinal thickness map shows some areas of increased retinal thickness corresponding to the fluid of the active CNV. (**f**) RPE map shows the irregularity of the RPE where the CNV membrane is placed. (**g**) The horizontal scan shows a fibrovascular RPE detachment, with the choroidal rupture subretinal and intraretinal fluid and posterior vitreous detachment (G)

In the second case, there was an irregular hyporeflective vertical failure corresponding to the choroidal rupture and a hyperreflective band radiating from the subretinal space through the entire neuroretina to the retinal surface, indicating a transretinal migration of fibrovascular cells (Fig. 27.10a, b).

27.5 Valsalva Retinopathy

The term "Valsalva retinopathy" was first used in 1972 by Duane to describe preretinal hemorrhages secondary to a sudden increase of intrathoracic pressure, in association after vomiting, coughing, heavy lifting, or straining stool, although in some instances no initiating event can be ruled out (Duane 1972). After the Valsalva maneuver, a sudden rise in the intraocular venous pressure causes retinal capillaries to spontaneously rupture; the consequence is the hemorrhage. A well-circumscribed, round, or dumbbell-shaped mound of preretinal blood is seen in or near the central macular area.

The most common site for this hemorrhage is the posterior pole, where the premacular bursa provides a preexisting anatomic space (Foos 1972). In addition the ILM (internal limiting membrane) has no firm attachments to the retina at the posterior pole, thus predisposing hemorrhagic detachments between both layers (Fig. 27.11a, b).

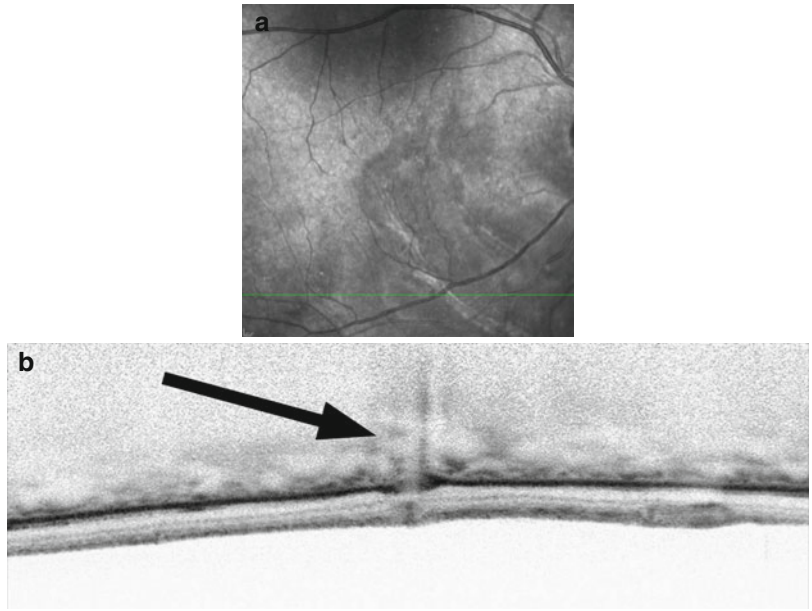

Fig. 27.10 (**a**) The red-free image shows a concentric whitish lesion in the inferior temporal area corresponding to the choroidal rupture. (**b**) The enhanced depth OCT imaging shows an irregular hyporeflective vertical lesion at the deep choroid corresponding the choroidal rupture (*arrow*). The retina has a normal thickness; however, there is a hyperreflective band extending from the outer retinal to throughout the entire retina to the retinal surface (Courtesy of Dr Daniel Lavinsky)

It is generally agreed that the sharply demarcated hemorrhage is located at the vitreoretinal interface either directly under the posterior hyaloid of the vitreous or under the internal limiting membrane (ILM) itself. The exact location of it cannot be determined biomicroscopically, although subhyaloid blood tends to shift by changing the head from an upright to flat position, and sublaminar retinal hemorrhage remains still (Choudhry and Rao 2014; Green et al. 1996) (Fig. 27.11c, d).

Patients commonly describe a sudden spontaneous loss of their vision. Part of the blood may decent in the preretinal bursa and turn yellow after several days. The prognosis is generally good, but resorption of the entrapped blood tends to be slow and may result in long-standing visual impairment. With a spontaneous rupture of the membrane, vision recovers rapidly. However, if the spontaneous resorption of preretinal blood is slow, laser puncturing or photodisruption of the posterior hyaloid face or the limiting membrane has been described by means of argon laser coagulation (Kroll and Busse 1986) or Nd:YAG laser (Ulbig et al. 1998) as an alternative to vitrectomy. The laser puncturing enables drainage through the focal opening of entrapped premacular blood into the vitreous cavity, where it is resorbed more quickly (Meyer et al. 2006).

Our group showed a patient that was submitted to focal membranotomy by argon laser and developed ERM with a superficial prominent sheen-like membrane. In these cases vitrectomy should be performed with ERM removal and ILM peeling with the use of vital dyes such as brilliant blue or indocyanine green for ILM and trypan blue for ERM (Meyer et al. 2004a; Schmidt et al. 2003). It has been shown that after performing a vitrectomy and histology in preretinal hemorrhages, it was possible to identify multiple layers of cells on the inside of the dome-shaped membrane (Garcia-Arumi et al. 1994).

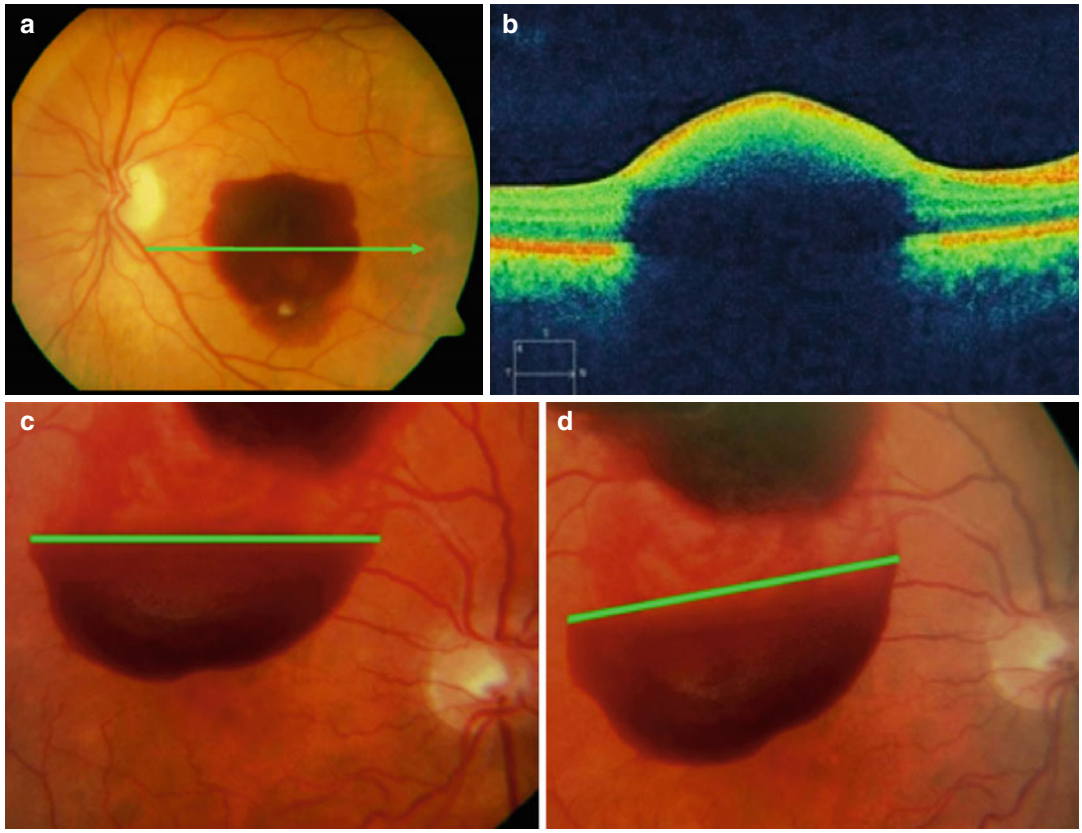

Fig. 27.11 Valsalva retinopathy. (**a**) Fundus image showing well-circumscribed, round, or dumbbell-shaped mound of preretinal blood in or near the central macular area. (**b**) The entrapped blood under the ILM presents on SD-OCT as hyperreflective band in the retina surface obscuring the underlying retinal structures. (**c**) Fundus image taken in an upright position. The preretinal hemorrhage has a horizontal direction. (**d**) Fundus image taken after the head was tilted to the right side. The preretinal blood has shifted to the right side in an oblique direction

27.6 Traumatic Optic Pit Maculopathy

Congenital pit of the optic nerve head is an excavation or regional depression of the optic nerve head resulting from an imperfect closure of the embryonic fissure. An unequal growth on both sides causes a delayed closure of the fissure at approximately 5 weeks of gestation. They were first described in 1882 as dark gray depressions in the optic nerve head, and they appear craterlike holes on the surface of the optic nerve head usually with a steep temporal wall, usually associated with posterior vitreous detachment and serous retinal detachment in the macular area (Kranenberg 1960).

The underlying mechanism optic pit maculopathy remains speculative, although many patients develop serous retinal detachments during life. As optic pits are congenital and the corresponding macular detachments develop later, certain unknown events may trigger macular detachments. It is known that most eyes with an optic pit maculopathy have a partial vitreous detachment (PVD) with firm attachments at the margin of the optic head (Sugar 1962). Therefore, one of the mechanisms that may trigger the serous detachment is the PVD associated or not with ocular trauma.

Many times, an optic pit is asymptomatic and is just an incidental finding on the examination of the eye by a physician. However, some patients may present with the symptoms of a posterior vitreous detachment or serous retinal detachment. This is because optic pits are associated with these disorders and are even speculated to be the actual cause of these disorders when they arise in patients with optic pits. The most common visual field defects include an enlarged blind spot and a scotoma. Visual acuity is typically not affected by the pit but may get worse if serous detachment of the macula occurs. Metamorphopsia may then result.

Funduscopy discloses a gray oval pit usually at the temporal margin of the disk (Fig. 27.12a). A shallow uniform opaque retinal detachment, about 4 disk diameters, extended from the edge of the optic nerve to the macula (Fig. 27.12a). OCT demonstrated an inner layer separation (ISL) with an outer layer detachment (OLD) of the retina (Fig. 27.12b). The non-reflective space between them corresponded to a large schisis-like cavity (Fig. 27.12b).

Lincoff et al. hypothesized a two-layered structure in optic pit maculopathy. The serous retinal elevations in optic pits primarily begin at the optic disk with a schisis-like separation of the inner retinal layers. The ILS appears clinically transparent, while the corresponding functional scotoma is mild and central vision may remain intact. When a hole in the outer layer develops, fluid may flow through into the subretinal space creating a secondary OLD (Lincoff and Kreissig 1998). Vigorous radial forces transmitted through abnormal vitreous attachment may have therefore exaggerate a schisis-like retinal detachment in our patients with a congenital optic pit (Meyer et al. 2003b; Meyer and Rodrigues 2004).

In general optic disk pits themselves do not need to be treated. However, patients with chronic serous retinal detachments with loss of visual acuity may be submitted to surgery. There are several case reports and case series treating those lesions with simple intravitreal gas injection or vitrectomy and fluid-gas exchange with functional and anatomical improvement with low

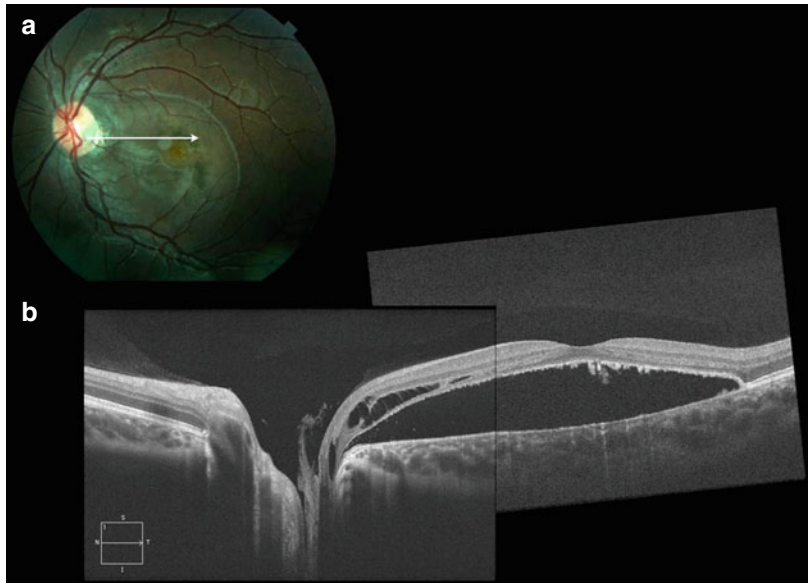

Fig. 27.12 Traumatic optic pit maculopathy. (**a**) Fundus picture shows an optic disk with a gray oval pit at the temporal side and a darker area in the papillomacular bundle (*arrow*). (**b**) The SD-OCT shows the pit inside the optic nerve head. In the papillomacular region, it is possible to observe an inner layer separation (ISL) in multiple layers. The outer layer detachment (OLD) of the neuroretina from the retinal pigment epithelium can be seen in a second hyperreflective band. The non-reflective space between the ILS and the OLD responds to a large schisis-like cavity. The RPE-choriocapillaris complex represents as a third hyperreflective band. The fluid under the OLD can leak through a hole in the outer layer into the subretinal space and the retinal schisis in multiple layers at the inner retina and subretinal fluid or a schisis in the outer retina (Courtesy of Dr Rodrigo Meirelles)

recurrence rates (Moreira Neto and Moreira Junior 2013; Akiyama et al. 2014).

27.7 Epiretinal Membrane

The proliferation of epiretinal membranes (ERMs) occurs spontaneously or as a complication of various diseases on the surface of the retina along the internal limiting membrane (ILM). Iwanoff first in 1865 considered ERM as the formation of endothelial cells (Iwanoff 1865). These cells mainly derive from retinal glial or RPE cell proliferating along the retinal surface and gain access to the ILM by unknown stimuli (Trese et al. 1983). The separation or peeling of ERM is a rare incidence. It may occur spontaneously without evidence of any intervention, by development of a PVD and Nd-YAG laser or after ocular trauma (Messner 1977).

Clinically ERMs are a semitransparent membrane that develops over the retina that may be asymptomatic or cause a contraction of the retinal tissue and consequent misalignment and damage to the retinal tissue (Fig. 27.13a). The final result is metamorphopsia, low visual acuity that may vary from almost normal to 20/400 or hand motion to the more severe and chronic cases. The diagnosis is clinical, but the use of SD-OCT is very important to the identification of the hyperreflective membrane on the retinal surface (Fig. 27.13b) and to the evaluation of the coexisting vitreoretinal traction that may be found in some cases (Fig. 27.14) (Bottós et al. 2012). Moreover the use of SD-OCT is also very important to evaluate the prognosis after surgery. It has been shown that edema of the inner retina correlates with poor prognosis and a disruption of the inner/outer segment layer (IS/OS) or the ellipsoid zone may also be associated with poor functional results after ERM removal (Fig. 27.15) (Kinoshita et al. 2012; Shiono et al. 2013).

The treatment for ERM is surgery; however, there are some reports of spontaneous ERM separation with visual acuity improvement (Meyer et al. 2004b). Usually vitrectomy is indicated when visual acuity is 20/40 or worse or if the patient has a remarkable metamorphopsia. Standard vitrectomy associated with ERM removal, with or without trypan blue staining, and today ILM peeling

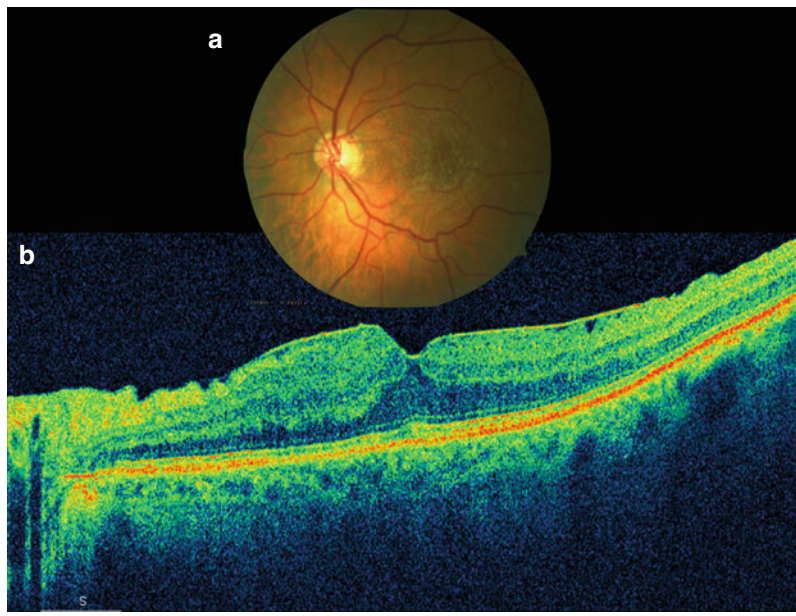

Fig. 27.13 Epiretinal membrane. (**a**) Fundus picture demonstrates loss of foveal reflex and the typical aspect of cellophane maculopathy. (**b**) Spectral domain OCT shows hyperreflective tissue over the retinal surface corresponding to the epiretinal membrane (ERM). There is an irregularity on the retinal surface and also some increase of the retinal thickness due to edema caused by the ERM

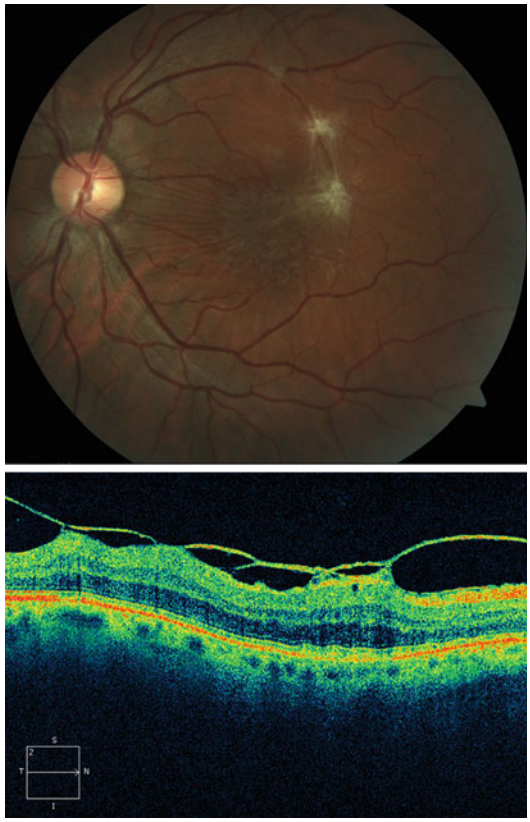

Fig. 27.14 Fundus picture and SD-OCT of a patient with vitreomacular traction and ERM. The first hyperreflective membrane is the vitreous traction and the second layer over the retinal surface is the ERM

with brilliant blue has also been performed to reduce the recurrence rate of ERM.

27.8 Traumatic Macular Hole

Macular hole (MH) can occur in either gender, at any age, with no racial predilection. The incidence in women is higher that may be attributed to the earlier onset of PVD due to premature vitreous liquefaction, probably associated with declining estrogen levels in the postmenopausal period. This profile is also seen in ERM, another condition considered to be a complication of PVD.

Vitreofoveal traction is believed to be important in the pathogenesis of idiopathic MH. Since Gass has described its early stages, the development of this pathology was attributed to tangential traction of the perifoveal vitreous cortex resulting in a foveal dehiscence that can progress from foveolar detachment to a mature full-thickness MH (Gass 1988, 1995). Some susceptible patients have abnormal and strong vitreomacular adherence, causing persistent foveal traction with perifoveal detachment, which is universally associated with the earliest MH stages. The continuous anterior traction of the slightly detached vitreous cortex appears to be a major contributing factor to MH formation. Both types of traction, anteroposterior and tangential, might be combined in some cases. Tangential traction may also be the result of glial cell proliferation onto the perifoveal internal limiting membrane and may explain the persistence and enlargement of MH, in some specific cases, even when the posterior hyaloid spontaneously detaches. The mechanisms of traumatic macular hole are slightly different from idiopathic MH. It has been postulated that it is formed by a necrotic cystoid degeneration of the foveal retinal tissue, associated with the subretinal hemorrhage and anterior vitreous traction.

Clinically the patients complain about loss of central vision, low visual acuity, and metamorphopsia. On the fundus exam, it is possible to identify a hole in the foveal area that could be confirmed on the slit lamp by the Watzke-Allen sign (Fig. 27.16a). With the fluorescein angiogram, it is possible to identify a hyperfluorescent lesion to the absence of the retinal tissue in the hole location. The spectral domain OCT may identify a true hole in the retina (Fig. 27.16b) and the presence of fluid in the edges, measure the size of the hole, and also evaluate the vitreoretinal interface to observe if the vitreous is still attached or the presence of ERM.

The main value of the SD-OCT is to help us understand the pathogenic theory (Fig. 27.17) and also clarify the possible therapeutic implications: a vitrectomy with the aim of resolving anteroposterior traction could be the main goal of a surgical procedure when the vitreous face is not totally separated from the edge of the MH. Otherwise, when no anteroposterior traction is shown by OCT or US, the surgeon would attempt to remove epiretinal tissue and internal limiting membrane to release the tangential traction. Moreover, the differentiation between VMT and PVD, by a

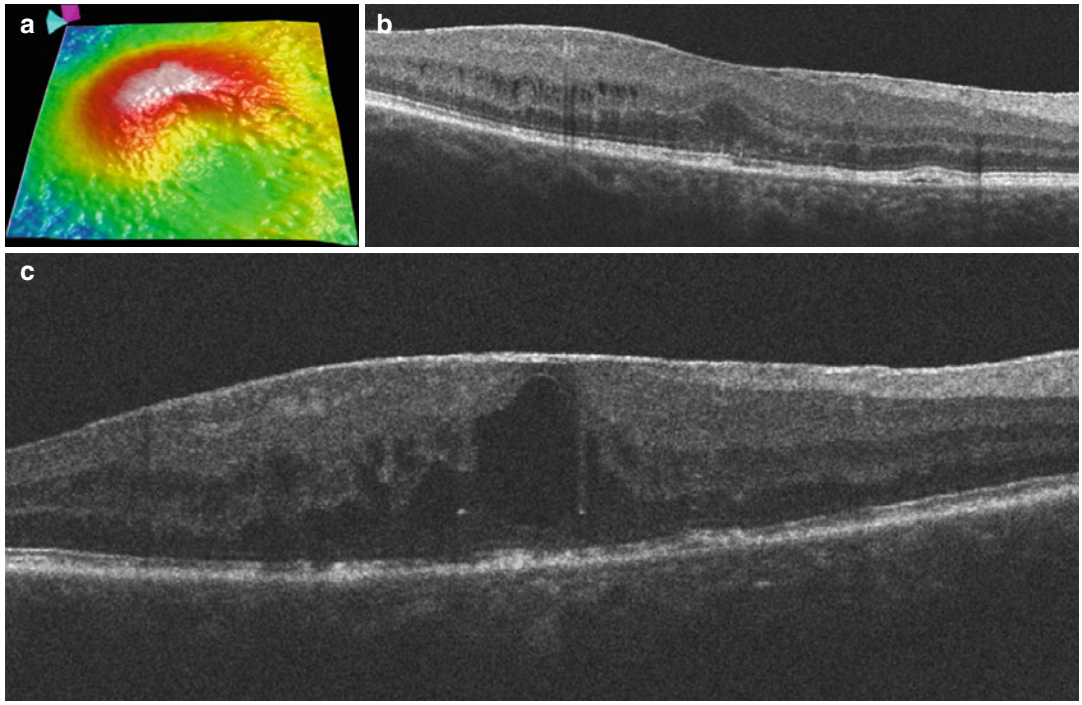

Fig. 27.15 In a patient with ERM at the initial presentation, the visual acuity was 20/50 with some increase in retinal thickness (**a**) and the SD-OCT scan shows a very adherent ERM with mild retinal edema (**b**). It was offered surgical treatment but the patient came back just 2 years later; now the visual acuity is 20/400 and the retinal anatomy is completely abnormal. Huge retinal cysts in the inner retina and disruption in the ellipsoid zone indicating a poor prognosis after surgery (**c**)

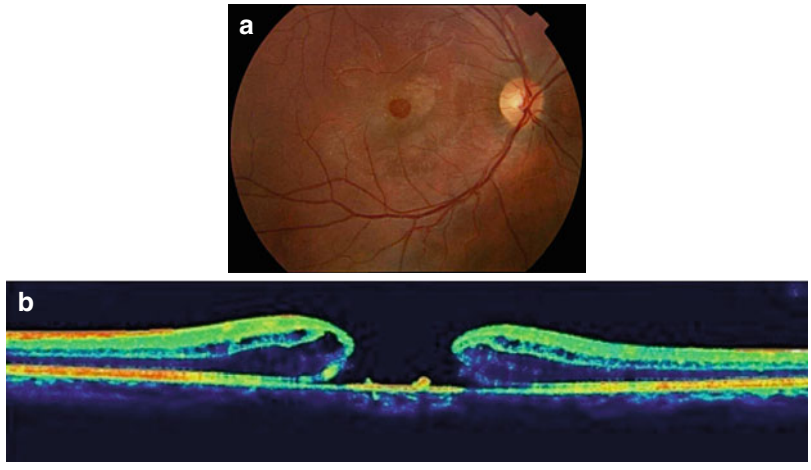

Fig. 27.16 Traumatic macular hole. (**a**) Fundus picture shows macular hole in the foveal area. (**b**) Spectral domain OCT showing complete disruption of all retinal layers revealing a macular hole. There are some cysts in the edges of the hole indicating a better prognosis after surgery

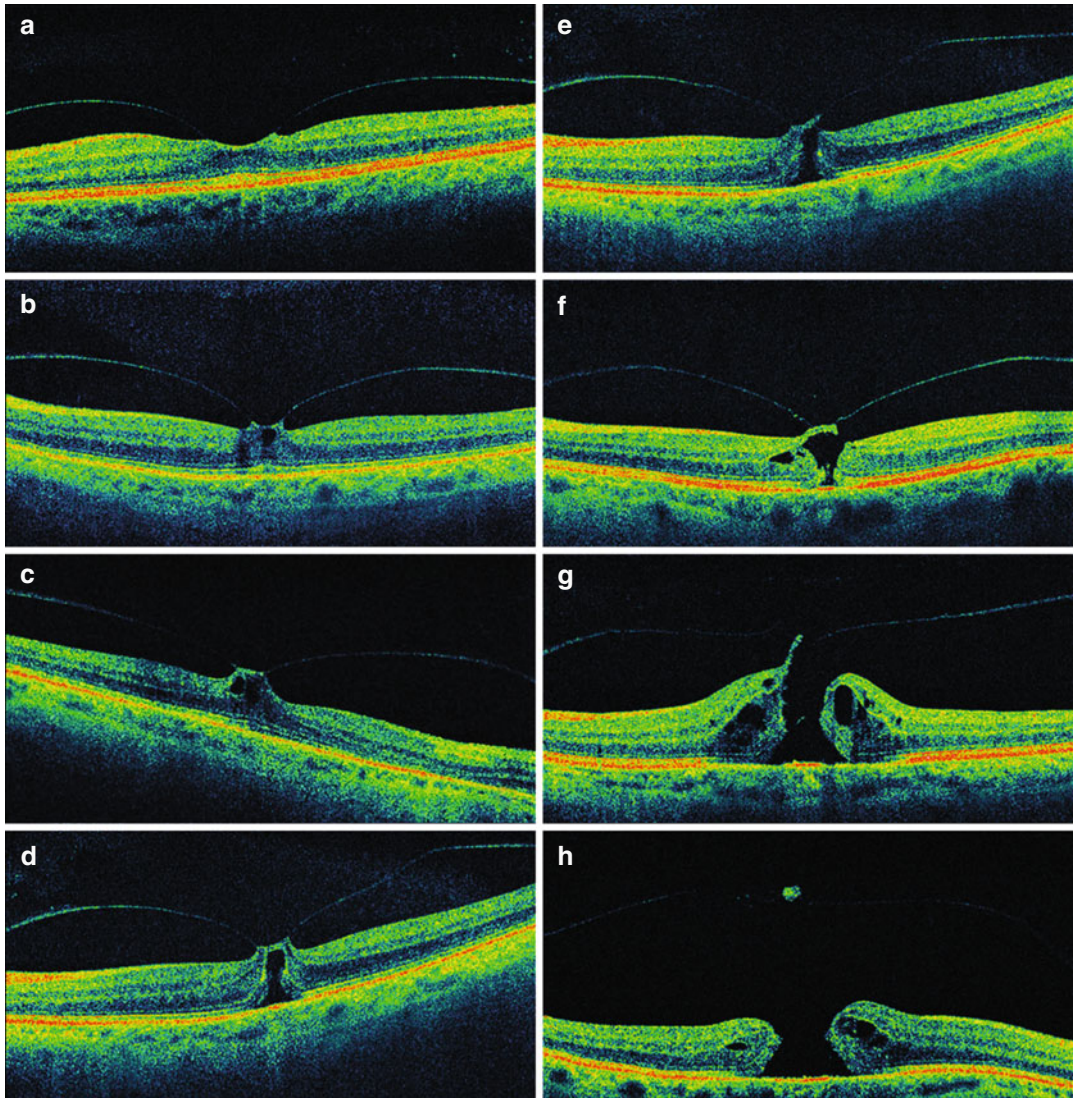

Fig. 27.17 Stages of macular hole. (**a**) SD-OCT shows that vitreous is still attached with almost no traction. (**b** and **c**) SD-OCT showing some anterior traction by the vitreous causing some changes in the retinal anatomy at the inner retina. (**d–h**) Showing evolution of the macular hole with progressive disruption of all retinal layers and enlargement of the hole and progressive release of the vitreous traction (Courtesy of Dr Juliana Bottós)

noninvasive technique, is inevitable and decisive for further surgical or pharmacological treatment.

Traumatic macular hole may close spontaneously but it also may require surgery (Yamashita et al. 2002). We describe a case of a 15-year-old boy that had a history of blunt ocular trauma due to a soccer ball. The initial visual acuity at his presentation 10 days after the trauma was 20/120 due to a traumatic macular hole. One month after the surgery, his visual acuity recovery was 20/60 with small amount of subretinal fluid that completely disappeared after 2 months, and his final visual acuity was 20/25 with a macular hole closure (Fig. 27.18).

27.9 Retinal Pigment Epithelium Tear

Retinal pigment epithelium tears occur most commonly in the posterior pole as a complication of age-related macular degeneration (AMD), and

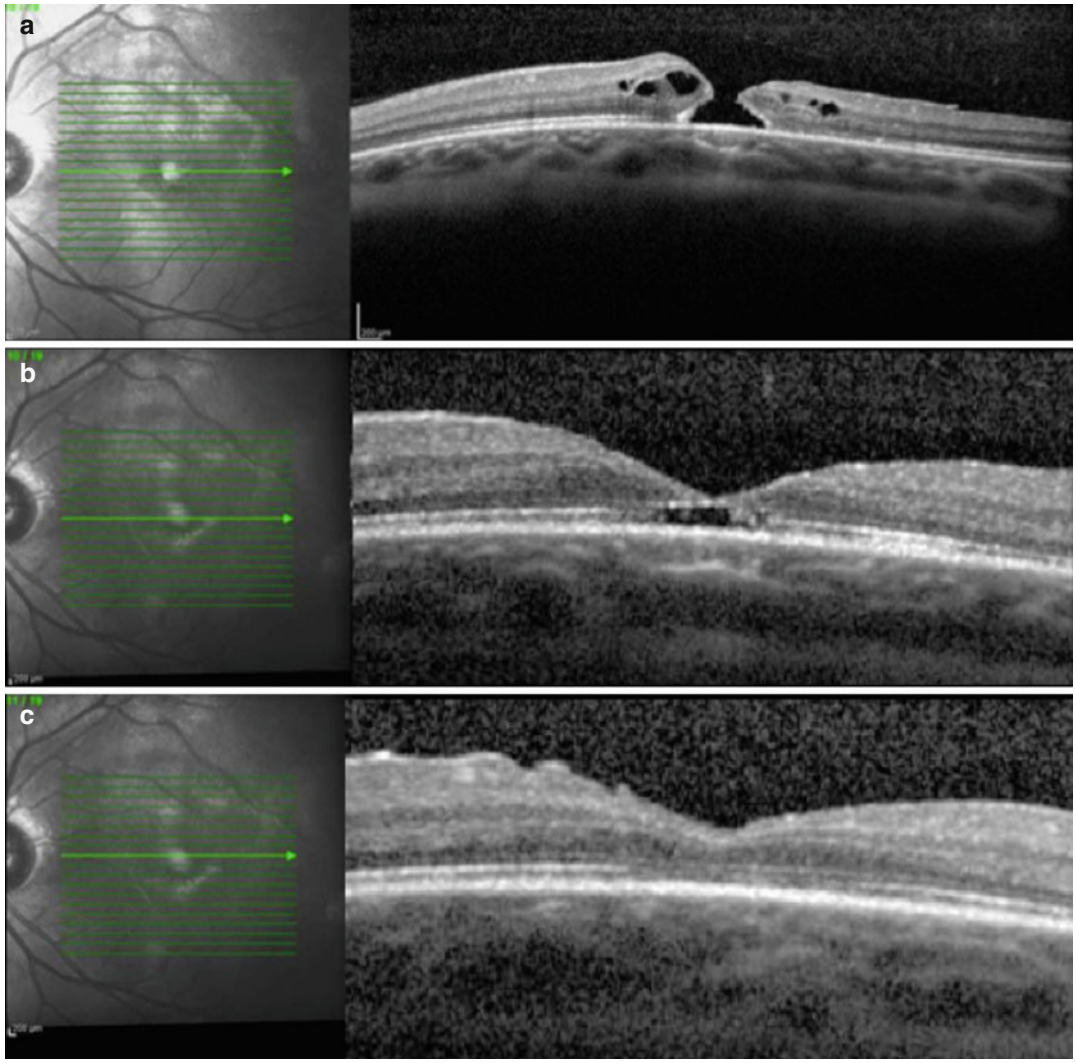

Fig. 27.18 Traumatic macular hole in a 15-year-old boy. (**a**) SD-OCT 10 days after the blunt ocular trauma shows full-thickness macular hole. (**b**) SD-OCT 1 month after the surgery shows small amount of subretinal fluid. (**c**) SD-OCT 2 months after the surgery shows complete disappearance of subretinal fluid and macular hole closure

it is generally associated with RPE detachments. RPE tears associated with blunt ocular trauma have been reported at the posterior pole and periphery (Doi et al. 2000; Levin et al. 1991). Levin et al. suggested that excessive force to the eye transmitting sufficient mechanical stress between the choroid and sclera and the RPE may induce RPE tears or choroidal ruptures (Levin et al. 1991).

We previously presented three patients with AMD and RPE tears in the presence of vitreomacular traction and postulated that shear and abnormal stresses from the vitreoretinal interface may trigger the development of RPE tears (Meyer and Toth 2001). Here we presented another case of a 68-year-old white man, who complained of low vision acuity. At presentation, his best-corrected VA was 20/23 OD and 20/400 OS. On biomicroscopy there was an area of subretinal elevation temporal to the fovea with hyperpigmentation superiorly consistent with folded RPE and CNV. Subretinal fluid extended superiorly and inferiorly to the lesion. The SD-OCT scan of the macula and the neurosensory retina was elevated as well as the RPE layer. It was possible to observe that the hyperreflective band correspondent to the

RPE was not continuous that was a failure corresponding to the tear. Adjacent to the reflective lesion was a well-demarcated area of low reflectivity in the subretinal space consistent with serous fluid. In the inner retina, it is possible to observe intraretinal cysts. The detached posterior hyaloid could be seen as a highly reflective band above the center of the fovea (Fig. 27.19).

27.10 Choroidal Excavation

Choroidal excavation or focal choroidal excavation (FCE) was first described in 2006, by Jampol et al., who reported a peculiar optical coherence tomography (OCT) finding in the macula, in which the choroid was excavated in an asymptomatic elderly woman (Jampol et al. 2006).

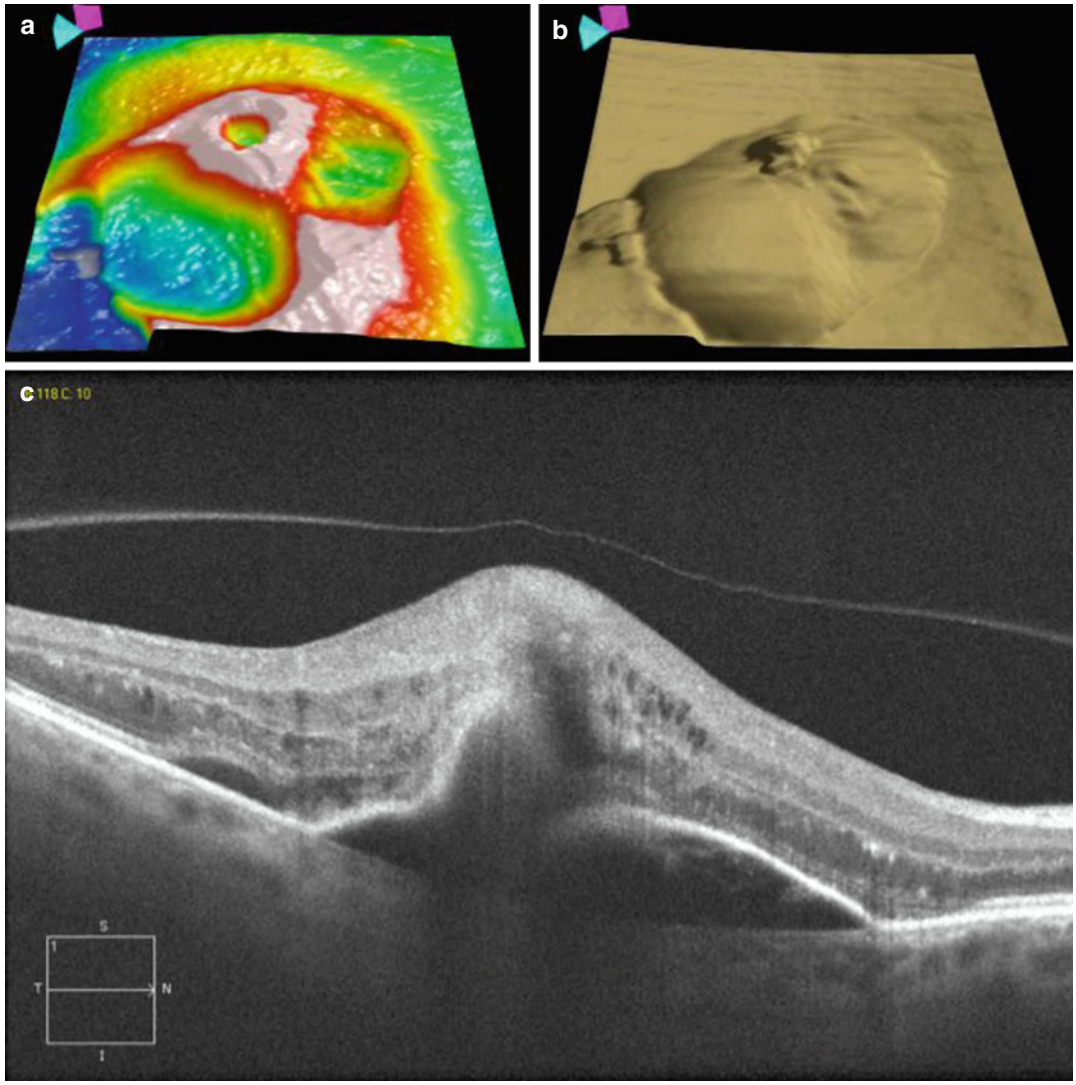

Fig. 27.19 Retinal pigment epithelium tear. (**a**) Spectral domain OCT shows subretinal fluid extending superiorly and inferiorly to the lesion that can be observed in the retinal thickness map. (**b**) The SD-OCT scan of the macula and the neurosensory retina is elevated as well as the RPE layer. (**c**) Shows noncontinuous hyperreflective RPE band corresponding to tear. Adjacent to the reflective lesion is a well-demarcated area of low reflectivity in the subretinal space consistent with serous fluid. In the inner retina, there are intraretinal cysts. The detached posterior hyaloid is seen as a highly reflective band above the center of the fovea

Later, Wakabayashi et al. identified three more patients with similar findings and called the lesions "unilateral choroidal excavation," because lesions were confined to only one eye (Wakabayashi et al. 2010). Margolis et al. found a bilateral case in their series of 12 patients and proposed the term "focal choroidal excavation" (FCE) (Margolis et al. 2011).

The cause of FCE is currently unknown. Occasional bilaterality and a relatively stable clinical course in the absence of any systemic or ocular conditions that may have disturbed the choroidal layer in the macula prompt investigators to suspect that FCE is a congenital abnormality. The clinical implications of FCE are largely unknown. Most patients appear to retain good visual acuity, but a few cases have been diagnosed with concurrent choroidal vascular disorders, including central serous chorioretinopathy (CSC), choroidal neovascularization (CNV), and polypoidal choroidal vasculopathy (PCV) (Lee et al. 2014).

We present a case of a 16-year-old woman complaining of a metamorphopsia and blurry vision for the last 4 months. She had a history of trauma 5 years ago. Her vision acuity was 20/40; in the fundus exam, it was possible to observe a grayish lesion temporal to the fovea with some pigmentary changes that correspond to a hyperfluorescent area on the fluorescein angiogram exam. The SD-OCT reveals a disruption of the outer retina and RPE with some fluid in the excavated area (Fig. 27.20). This is a case of a secondary CNV associated with FCE in a patient with ocular trauma in the past that was treated with anti-vascular endothelial growth factor intravitreal injections with good functional and anatomical recovery.

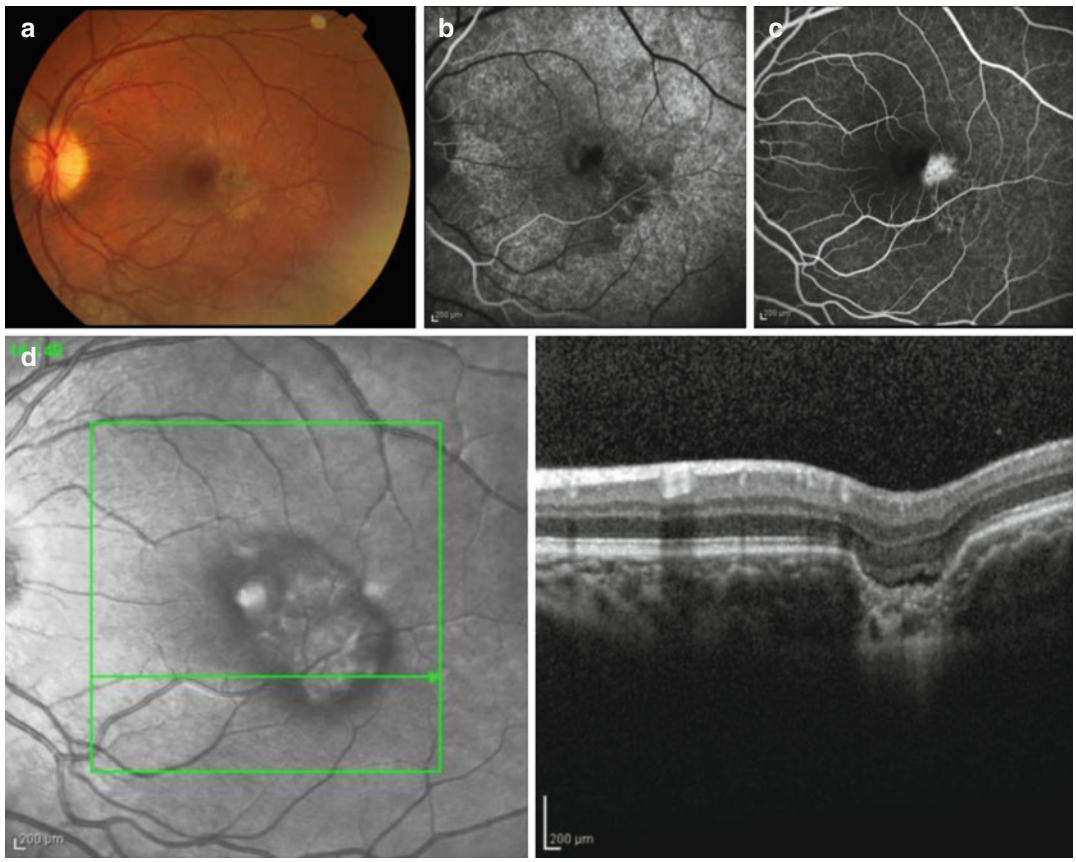

Fig. 27.20 Choroidal excavation. (**a**) The color fundus image shows a grayish lesion temporal to the fovea with some pigmentary changes. (**b**, **c**) The corresponding lesion is hyperfluorescent on fluorescein angiogram. (**d**) The SD-OCT reveals a disruption of the outer retina and RPE with some fluid in the excavated area

References

Akiyama H, Shimoda Y, Fukuchi M, Kashima T, Mayuzumi H, Shinohara Y, Kishi S (2014) Intravitreal gas injection without vitrectomy for macular detachment associated with an optic disc pit. Retina 34:222–227

Berg P, Kroll P, Krause K (1989) Pathogenic mechanism of contusio bulbi. Fortschr Ophthalmol 86:407–410

Berlin R (1873) Zur sogenannten commotio retinae. Klin Monatsbl Augenheilkd 1:42–78

Bottós JM, Elizalde J, Rodrigues EB, Maia M (2012) Current concepts in vitreomacular traction syndrome. Curr Opin Ophthalmol 23:195–201

Choudhry N, Rao RC (2014) Images in clinical medicine: valsalva retinopathy. N Engl J Med 370:1368

Dailey RA, Mills RP, Stimac GK, Shults WT, Kalina RE (1986) The natural history and CT appearance of acquired hyperopia with choroidal folds. Ophthalmology 93:1336–1342

Doi M, Osawa S, Sasoh M, Uji Y (2000) Retinal pigment epithelial tear and extensive exudative retinal detachment following blunt trauma. Graefes Arch Clin Exp Ophthalmol 238:621–624

Duane TD (1972) Valsalva retinopathy. Trans Am Ophthalmol Soc 70:298–311

Dubovy SR, Guyton DL, Green WR (1997) Clinicopathologic correlation of chorioretinitis sclopetaria. Retina 17:510–520

Fernández MG, Navarro JC, Castaño CG (2012) Long-term evolution of Valsalva retinopathy: a case series. Journal of medical case reports 6:1

Foos RY (1972) Vitreoretinal juncture, topographical variations. Invest Ophthalmol 11:801–809

Garcia-Arumi J, Corcostegui B, Tallada N, Salvador F (1994) Epiretinal membranes in tersons syndrome. A clinicopathologic study. Retina 14:351–355

Gass JD (1988) Idiopathic senile macular hole. Its early stages and pathogenesis. Arch Ophthalmol 106:629–639

Gass JD (1995) Reappraisal of biomicroscopic classification of stages of development of a macular hole. Am J Ophthalmol 119:752–759

Green MA, Lieberman G, Milroy CM, Parsons MA (1996) Ocular and cerebral trauma in non-accidental injury in infancy: underlying mechanisms and implications for paediatric practice. Br J Ophthalmol 80:282–287

Hesse L, Bodanowitz S, Kroll P (1996) Retinal necrosis after blunt ocular trauma. Klin Monatsbl Augenheilkd 209:150–152

Iwanoff A (1865) Beiträge zur normalen und pathologischen Anatomie des Auges. Archiv für Ophthalmologie 11:135–170

Jampol LM, Shankle J, Schroeder R et al (2006) Diagnostic and therapeutic challenges. Retina 26:1072–1076

Janknecht P (2011) Treatment of traumatic choroidal neovascularization with ranibizumab. Ophthalmology 108:57–59

Kinoshita T, Imaizumi H, Okushiba U, Miyamoto H, Ogino T, Mitamura Y (2012) Time course of changes in metamorphopsia, visual acuity, and OCT parameters after successful epiretinal membrane surgery. Invest Ophthalmol Vis Sci 53:3592–3597

Kranenberg EW (1960) Crater-like holes in the optic disc and central serous retinopathy. Arch Ophthalmol 64:912–924

Kroll P, Busse H (1986) Therapy of preretinal macular hemorrhages. Klin Monatsbl Augenheilkd 188: 610–612

Lee CS, Woo SJ, Kim YK et al (2014) Clinical and spectral-domain optical coherence tomography findings in patients with focal choroidal excavation. Ophthalmology 121:1029–1035

Levin LA, Seddon JM, Topping T (1991) Retinal pigment epithelial tears associated with trauma. Am J Ophthalmol 112:396–400

Lincoff H, Kreissig I (1998) Optic coherence tomography of pneumatic displacement of optic disk pit maculopathy. Br J Ophthalmol 83:367–372

Mansour AM, Green WR, Hogge C (1992) Histopathology of commotio retinae. Retina 12:24–28

Margolis R, Mukkamala SK, Jampol LM et al (2011) The expanded spectrum of focal choroidal excavation. Arch Ophthalmol 129:1320–1325

Mennel S, Meyer CH, Kroll P (2004) Dislocation of the lenses. N Engl J Med 351:1913–1914

Mennel S, Hausmann N, Meyer CH, Peter S (2005) Photodynamic therapy and indocyanine green guided feeder vessel photocoagulation of choroidal neovascularization secondary to choroidal rupture after blunt trauma. Graefes Arch Clin Exp Ophthalmol 243:68–71

Messner KH (1977) Spontaneous separation of preretinal macular fibrosis. Am J Ophthalmol 83:9–11

Meyer CH, Rodrigues EB (2004) Optic disc pit maculopathy after blunt ocular trauma. Eur J Ophthalmol 14:71–73

Meyer CH, Toth CA (2001) Retinal pigment epithelial tear with vitreomacular attachment: a novel pathogenic feature. Graefes Arch Clin Exp Ophthalmol 239:325–333

Meyer CH, Rodrigues EB, Mennel S (2003a) Acute commotio retinae determined by cross-sectional optical coherent tomography. Eur J Ophthalmol 13:816–818

Meyer CH, Rodrigues EB, Schmidt JC (2003b) Congenital optic nerve head pit associated with reduced retinal nerve fiber thickness at the papillomacular bundle. Br J Ophthalmol 87:1300–1301

Meyer CH, Rodrigues EB, Kroll P (2004a) Reduced concentration and incubation of intravitreal Indocyanine green can improve the functional outcome in macular hole surgery. Am J Ophthalmol 137:386

Meyer CH, Rodrigues EB, Mennel S, Schmidt JC, Kroll P (2004b) Spontaneous separation of epiretinal membrane in young subjects: personal observations and review of the literature. Graefes Arch Clin Exp Ophthalmol 242:977–985

Meyer CH, Mennel S, Rodrigues EB, Schmidt JC (2006) Persistent premacular cavity after membranotomy in

Valsalva retinopathy on optical coherence tomography. Retina 26:116–118
Moreira Neto CA, Moreira Junior CA (2013) Vitrectomy and gas-fluid exchange for the treatment of serous macular detachment due to optic disc pit: long-term evaluation. Arq Bras Oftalmol 76:159–162
Nettleship E (1884) Peculiar lines in the choroid in a case of post-papillitic atrophy. Trans Ophthalmol Soc UK 4:167
Norton EWD (1969) A characteristic fluorescein angiographic pattern in choroidal folds. Proc R Soc Med 62:119
Pahor D (2000) Changes in retinal light sensitivity following blunt ocular trauma. Eye 14:583–589
Piermarocchi S, BenettiE FG (2011) Intravitreal bevacizumab for posttraumatic choroidal neovascularization in a child. J AAPOS 15:314–316
Schmidt JC, Meyer CH, Rodrigues EB, Hörle S, Kroll P (2003) Staining of the internal limiting membrane in vitreoretinal surgery: a simplified technique. Retina 23:263–264
Secretan M, Sickenberg M, Zografos L, Piguet B (1998) Morphometric characteristics of traumatic choroidal ruptures associated with neovascularization. Retina 18:62–66
Shiono A, Kogo J, Klose G, Takeda H, Ueno H, Tokuda N, Inoue J, Matsuzawa A, Kayama N, Ueno S, Takagi H (2013) Photoreceptor outer segment length: a prognostic factor for Idiopathic epiretinal membrane surgery. Ophthalmology 120:788–794
Sipperley JO, Quigley HA, Gass DM (1978) Traumatic retinopathy in primates. The explanation of commotio retinae. Arch Ophthalmol 96:2267–2273
Sugar HS (1962) Congenital pits in the optic disc with acquired macular pathology. Am J Ophthalmol 53:307–311
Trese M, Chandler D, Machemer R (1983) Macular pucker. I Prognostic criteria. Graefes Arch Clin Exp Ophthalmol 221:12–15
Ulbig MW, Mangouritsas G, Rothbacher HH, Hamilton AM, McHugh JD (1998) Long-term results after drainage of premacular subhyaloid hemorrhage into the vitreous with a pulsed Nd:YAG laser. Arch Ophthalmol 116:1465–1469
Von Graefe A (1854) Zwei Fälle von Ruptur der Choroidea. Graefes Arch Clin Exp Ophthalmol 1:402
Wagemann A (1902) Zur pathologischen Anatomie der Aderhautruptur und Iridodialyse. Bericht Deutsche Ophthal Ges 30:278–282
Wakabayashi Y, Nishimura A, Higashide T et al (2010) Unilateral choroidal excavation in the macula detected by spectral-domain optical coherence tomography. Acta Ophthalmol 88:e87–e91
Williams DF, Mieler WF, Williams GA (1990) Posterior segment manifestations of ocular trauma. Retina 10(Suppl 1):S35–S44
Yamashita T, Uemara A, Uchino E, Doi N, Ohba N (2002) Spontaneous closure of traumatic macular hole. Am J Ophthalmol 133:230–235